Evidence of a 4–6 Day Barotropic, Planetary Oscillation of the Pacific Ocean

DOUGLAS S. LUTHER

Scripps Institution of Oceanography, University of California, San Diego, A-025, La Jolla, CA 92093

(Manuscript received 2 October 1981, in final form 9 April 1982)

ABSTRACT

Spectral analysis of scattered island and coastal tide-gage records from the Pacific Ocean reveals the presence of a coherent sea level fluctuation at 4–6 days period. The oscillation is distinct from baroclinic, inertia-gravity wave fluctuations of sea level at the same periods that are trapped to the central Pacific equatorial zone. Concomitant spectral analysis of island surface weather data demonstrates that sea level is forced by surface atmospheric pressure but does not respond statically like an "inverted barometer". The basinwide character and uniform westward propagation of the oscillation suggest the presence of a barotropic, planetary wave(s). However, the oscillation is strongly attenuated, with an estimated energy *e*-folding time of less than three days.

1. Introduction

Atmospherically-forced planetary oscillations may be responsible for considerable large-scale oceanic variability in the period range of days to months over large areas of the world's oceans, especially, but not exclusively, in regions devoid of strong mean currents (Frankignoul and Müller, 1979; Willebrand *et al.*, 1980; Müller and Frankignoul, 1981). Estimates of the magnitudes of the atmospherically-generated oscillations have frequently been made by simple summations of basin modes forced by oscillatory winds (Phillips, 1966; Leetmaa, 1978), but the technique suffers from a sensitivity to the dissipation parameter (Harrison, 1979), a problem which also occurs in numerical models. Willebrand *et al.*'s (1980) numerical study of oceanic response to realistic, stochastic atmospheric forcing found barotropic, basinwide, planetary mode resonances in the flat-bottomed model which were replaced by smaller-scale topographically-trapped, resonant oscillations in the rough-bottomed model. This well-known effect of topography on planetary oscillations (e.g., Rhines and Bretherton, 1973) is often considered the reason for the lack of observations of basin-wide, barotropic, planetary modes in the oceans.

During the course of a study of equatorially-trapped, inertia-gravity waves, high coherence amplitude among Pacific Ocean sea level records was found ubiquitously in the 4–6 day band. Evidence is presented here showing that sea level fluctuations in the 4–6 day band, outside the central Pacific equatorial waveguide, are dominated by a relatively narrow-band (in frequency and wavenumber), barotropic oscillation that appears to be predominantly a planetary mode. The estimate of the dissipation time scale of this mode can be used as a constraint in the theoretical models of atmospherically-forced planetary oscillations.

The theory of equatorially-trapped waves (e.g., Matsuno, 1966; Moore and Philander, 1977) defines a narrow zonal band about the equator, poleward of which the oscillations are evanescent. For example, the theory predicts that for the low-mode inertia-gravity waves identified by Wunsch and Gill (1976), which produce the 3-, 4- and 5-day peaks in the sea-level spectrum from Christmas Island (Fig. 1), the power in the sea-surface displacement of these waves at ±13° of latitude will be less than 1% of the maximum power near the equator. The surprise, then, was finding strong coherence amplitude at 4–6 day periods between sea level stations far from the equator, for example, between Eniwetok Atoll (11°21′N, 162°21′E) and Wake Island (19°17′N, 166°39′E) (Fig. 2).

The oceanic oscillation responsible for the high, sea level coherence amplitude in the 4–6 day band, outside the central-Pacific equatorial waveguide, is found to be a non-static response to forcing by the surface air pressure field (Section 3). The hypothesis that the oceanic oscillation is predominantly a barotropic, planetary mode of the Pacific is advanced in Section 4, where previous observational and theoretical work on planetary modes of the Pacific is reviewed. The planetary mode hypothesis is tested in Section 5, where estimates are presented of the propagating component of the mode. Estimates of amplitude and frequency bandwidth are discussed in Section 6. The observations are summarized in Section 7, and Section 8 concludes this paper with discussion, caveats and plans for further research.

0022-3670/82/070644-14$07.50

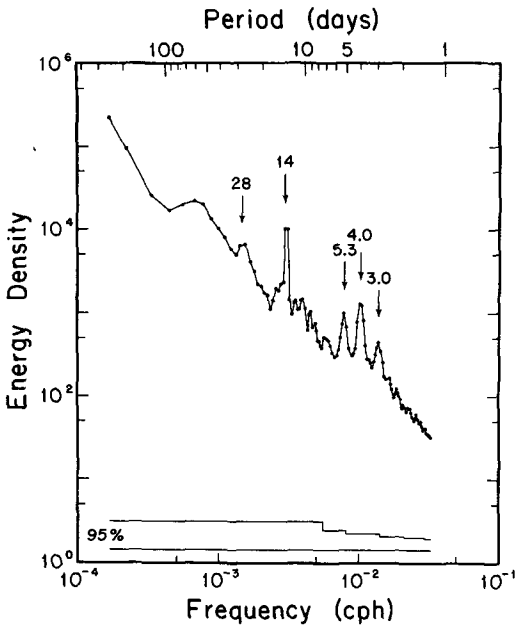

FIG. 1. Power spectrum of 15.4 years of sea-level data from Christmas Island (2°0'N, 157°30'W). The 3-, 4- and 5-day peaks are due to low-mode inertia-gravity waves. The peaks at 14 and 28 days are due to the tides. The ordinate is in units of $(cm)^2$/cph. Normalization is such that the power of a unit amplitude sine wave is 1. The 95% confidence intervals for each independent estimate are at the bottom of the figure. Every other point plotted is independent, i.e., there is 50% overlap of averaged frequency bands.

2. Datasets and analysis procedures

a. Sea level data

The sea level data consist of tide-gage records that have been assembled from a variety of sources over the past 15 years, especially the Institute of Geophysics and Planetary Physics (La Jolla), the National Ocean Survey, and Klaus Wyrtki (University of Hawaii). Much of the data was obtained under the direction of Carl Wunsch at the Massachusetts Institute of Technology.

The sea level time series range in length from less than one year to over twenty years (Table 1) and are scattered, not very uniformly, across the Pacific Ocean (Fig. 3). The temporal overlap is seen to be quite irregular, limiting the possible cross-spectra that can be computed, and requiring the *a priori* assumption of stationarity of the 4–6 day oscillation through three decades.

All records are hourly samples rounded to the nearest 0.1 ft, at worst, with some records rounded to the nearest 0.1 cm. Errors due to this "least count" roundoff and errors due to instrumental frequency response characteristics and drift have been discussed by Wunsch (1966) for a subset of the data used here. The possible errors are negligible for periods greater than 2 days.

Some of the records have been edited with rather sophisticated error detection and replacement schemes (Wunsch, 1966), but most have simply been subjectively scanned for obviously "bad" points and gaps. Single "bad" points and 1–2 h gaps were filled by linear interpolation. For larger gaps (at most several days), the tidal signal was predicted by the harmonic method and adjusted for the long-period trends surrounding the gap. Much larger gaps were not filled and were subsequently avoided.

Further error detection (with subsequent correction) occurred via the computation of tidal harmonic constants which were compared with published values (e.g., Special Publication No. 26 of the International Hydrographic Bureau, Monaco). The harmonic constants are sensitive to subtle errors in the timing of the records. At worst, errors that have escaped detection will degrade the cross-spectra, so we have erred on the side of caution.

The question of whether island sea level measurements are representative of open ocean conditions has been addressed by Wunsch (1972), Luther and Wunsch (1975) and others. For instance, positioning a tide gage within a lagoon that has restricted communication with the open ocean can produce sea level records that differ substantially from the sea level

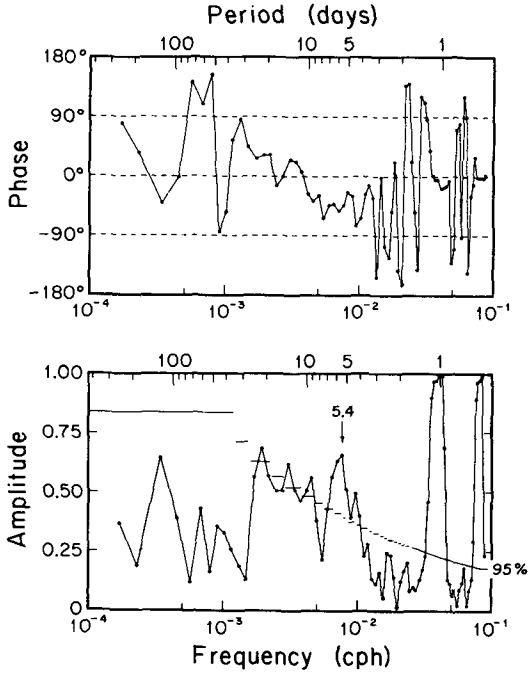

FIG. 2. Coherence amplitude and phase between two years of sea-level data from Eniwetok (11°21'N, 162°21'E) and Wake (19°17'N, 166°39'E); note the high amplitude at 4–6 days. Only the semidiurnal, diurnal and fortnightly tidal peaks are well understood. The 95% level of no significance for each independent amplitude estimate is indicated. Every other point plotted is independent, i.e., there is 50% overlap of averaged frequency bands. Positive phase indicates the first station (Eniwetok) leads.

TABLE 1. (Part 1). Locations and time intervals of sea level records—Pacific Ocean.*

Station	Latitude (degrees, minutes)	Longitude	Years of data	1948 1949 1950 1951 1952 1953 1954 1955 1956 1957 1958 1959 1960 1961 1962 1963 1964 1965 1966 1967 1968 1969 1970 1971 1972 1973 1974 1975 1976
Balboa	8 57 N	79 34 W	8.1	XXXXXXXXXXXX
Buenaventura	3 54 N	77 05 W	4.1	XXXXXXX
La Libertad	2 12 S	80 55 W	4.1	XXXXXXX
Talara	4 35 S	81 17 W	4.8	XXXX XXXX
Galapagos	0 54 S	89 34 W	7.2	XXXXXXXXXXX
Christmas Is.	2 00 N	157 30 W	15.6	XXXXXXXXXXX XXXXXXXXXX XXX
Fanning Is.	3 54 N	159 24 W	2.8	XXX XXX
Jarvis Is.	0 23 S	160 02 W	0.3	X
Canton Is.	2 49 S	171 40 W	19.9	XXXXXXXXXXXXXXXXXXXXXXXXXX XXX
Hull Is.	4 30 S	172 07 W	0.8	X
Arorae Is.	2 37 S	176 50 E	2.1	XXXX
Betio Is.	1 22 N	172 56 E	2.8	XXXX
Ocean Is.	0 53 S	169 35 E	2.2	XXXX
Nauru	0 32 S	166 55 E	2.0	XXXX
Rabaul	4 12 S	152 11 E	2.1	XXX
Dreger Hbr.	6 39 S	147 52 E	1.4	XXX
Jabor	5 55 N	169 39 E	0.3	X
Majuro At.	7 10 N	171 05 E	2.2	XXXX
Kwajalein	8 44 N	167 44 E	9.9	XXXXXXXXXXX XXXX
Eniwetok	11 21 N	162 21 E	9.1	XXX XXXXXXXX XXXX
Ponape Is.	7 00 N	158 15 E	1.7	XXX
Satawan	5 16 N	153 39 E	0.8	XX
Truk	7 27 N	151 52 E	6.7	XXXXXXXX XXXX
Puluwat Is.	7 22 N	149 13 E	0.8	XX
Yap Is.	9 30 N	138 10 E	1.6	XXX
Malakal Hbr.	7 19 N	134 27 E	1.3	XX
Guam	13 27 N	144 39 E	6.5	XXXXXXXX XX
Wake Is.	19 17 N	166 39 E	5.6	XXXXXXX XX
Johnston Is.	16 45 N	169 32 W	7.2	XXXXXXXX XXXX
Pago Pago Hbr.	14 17 S	170 40 W	3.1	XX XXXX
Hilo	19 42 N	155 04 W	12.7	XXXXXXXXXXXXXXX XXXX
Kahului	20 56 N	156 29 W	7.0	XXXXXXXXXX
Honolulu	21 19 N	157 52 W	36.6	1921→XXXXXXXXXXX XXX
Nawiliwili	21 57 N	159 21 W	4.1	XXX X XX
Midway Is.	28 12 N	177 22 W	7.2	XXXXXXXX XXXX
San Francisco	37 48 N	122 28 W	12.3	XXXXXXXXXXXXXXXXXX
Massacre Bay	52 50 N	173 12 E	8.7	XXXXXXXXXXXXX

* X's indicate data.

fluctuations of the surrounding ocean, due to thermal expansion in the lagoon, surf set-up and slow response time to outside sea level changes. In addition, important differences in sea level measured on opposite sides of an island can occur due to impinging currents (Hogg, 1972; Hendry and Wunsch, 1973) and diffraction of long ocean waves by island arcs (Larsen, 1977), etc. For the 4–6 day band, only diffraction may be important in the interpretation of the following analyses. The other processes contribute to what we consider here to be the "noise" energy, but we do not expect this locally-derived "noise" to dominate the 4–6 day band.

b. Surface weather data

Measurements of atmospheric variables (wind velocity, pressure and temperature) near sea level from island platforms have been obtained from the National Climatic Center, either in Tape Data Format 13 (TDF-13) or TDF-14. The TDF-13 data generally consist of at least three observations per day and the TDF-14 data are usually hourly samples. The datasets typically span four years or more and required only superficial editing for obviously bad points. Some pertinent information for the stations is listed in Table 1 (see Fig. 3 for the geographical distribution).

Enough observations per day were collected at all stations to avoid aliasing from diurnal activity, either tidal oscillations or thermally-generated "sea breezes", although most of the islands do not contain enough land area to generate strong daily sea breezes.

As for the sea level measurements, there is a question as to whether meteorological measurements from mid-ocean islands are representative of open ocean conditions. This problem can be regarded as

a matter of degree depending on the variable, the topography of the island, vegetation, man-made obstacles, and the location and height of the instruments. [Hwang (1970) and Wyrtki and Meyers (1975) have examined this problem with respect to the winds with limited datasets.] Only surface air pressure, which of the four weather variables is affected least by the island environment (Ramage *et al.*, 1980), is important in the present study, so a detailed discussion of the effects of the island environments on the weather spectra is deferred to a later paper. In any case, the island weather data are evaluated in toto, not singly. Considering the wide variety of island environments, it is unlikely that unique island effects, even if present in individual power spectra, would affect the cross-spectra between stations in a manner that would increase coherence. (Exceptions to this last statement may occur for diurnal phenomena, such as sea breezes, which are narrow-band and relatively phase-locked.)

c. *Analysis procedures*

Standard techniques are employed for estimating power spectra, coherence functions and wavenumber spectra. Power spectra are computed by removing the mean, tapering with a half-cycle cosine filter applied to 10% of the data length at each end, fast-Fourier transforming the tapered series, band-averaging equally-weighted periodogram estimates and, finally, correcting for the reduction of variance due to the tapering procedure (i.e., the spectral estimates are multiplied by 1/0.873). The width of the averaged frequency band is allowed to increase with frequency to improve statistical reliability while maintaining adequate resolution. If a record exists in more than one piece, the above procedure is applied to each piece, and the spectra are then averaged. The spectra are normalized so that the power of a unit amplitude sine wave is 1. The confidence intervals have been adjusted for the reduction of variance due to the tapering procedure. [The procedures outlined above are a combination of those discussed by Bingham *et al.* (1967) and Madden and Julian (1971) among others.]

The coherence function and gain are computed from auto- and cross-spectra that are calculated in a manner equivalent to that just described for auto-spectra.

The high-resolution (maximum-likelihood) wavenumber spectrum is calculated following the method introduced by Capon (1969). [See Wunsch and Hendry, (1972) for an oceanographic application of the maximum-likelihood wavenumber spectrum and a summary of the computational procedure, discussion of aliasing, etc.] Confidence intervals were computed following the analysis of Capon and Goodman (1970).

TABLE 1. (Part 2). Locations and time intervals of surface weather records—Pacific Ocean.

Station	Latitude (degrees, minutes)	Longitude	Number of observations per day	Years of data	1941	1942	1943	1944	1945	1946	1947	1948	1949	1950	1951	1952	1953	1954	1955	1956	1957	1958	1959	1960	1961	1962	1963	1964	1965	1966	1967	1968	1969	1970	1971	1972	1973	1974	1975	1976	1977	1978
Balboa	8 57 N	79 34 W	24	13.7				X	X	X	X	X	X	X	X	X	X	X	X	X	X	X	X	X	X	X	X	X	X	X	X										
Galapagos	0 54 S	89 37 W	3–7	5.0																											X	X	X	X	X							
Canton	2 46 S	171 43 W	8–24	17.9																																						
Arorae	2 40 S	176 50 E	3	3.6																X	X	X	X	X																		
Betio	1 21 N	172 55 E	2–3	9.2																X	X	X	X	X	X	X	X	X	X	X											
Ocean	0 54 S	169 32 E	2–3	4.6																				X	X	X	X	X	X	X											
Majuro	7 5 N	171 23 E	7–24	23.9																				X	X	X	X	X	X	X	X	X	X	X	X	X	X	X	X	X	X
Kwajalein	8 44 N	167 44 E	24	4.0																X	X	X	X	X																	
Eniwetok	11 21 N	162 21 E	24	4.0																X	X	X	X	X																	
Ponape	6 58 N	158 13 E	6–24	3.7																X	X	X	X	X	X	X	X	X	X	X											
Truk	7 28 N	151 51 E	4–24	27.5																				X	X	X	X	X	X	X	X	X	X	X	X	X	X	X	X	X	X
Yap	9 30 N	138 7 E	4–24	27.5																				X	X	X	X	X	X	X	X	X	X	X	X	X	X	X	X	X	X
Guam	13 30 N	144 48 E	24	4.0																X	X	X	X	X																	
Wake	19 17 N	166 39 E	24	4.0																X	X	X	X	X																	
Johnston	16 44 N	169 31 W	8–24	19.6																										X	X	X	X	X	X	X	X	X	X	X	X
Pago Pago	14 20 S	170 43 W	8	12.8																																					X
Hilo	19 43 N	155 4 W	24	4.0																X	X	X	X	X																	
Honolulu	21 20 N	157 55 W	24	14.6				X	X	X	X	X	X	X	X	X	X	X	X	X	X	X	X	X																	
Midway	28 12 N	177 23 W	24	4.0																X	X	X	X	X																	

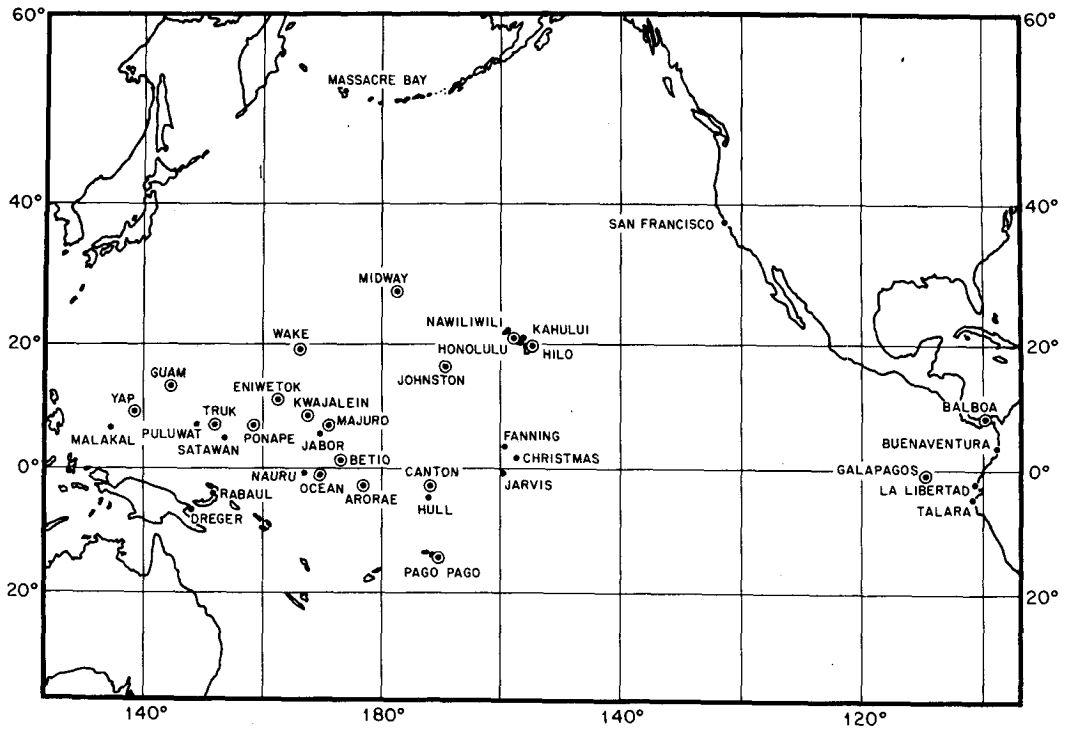

FIG. 3. Map of the Pacific Ocean showing locations of the tide gage and weather stations supplying data for use in this study. Weather stations are indicated by circles.

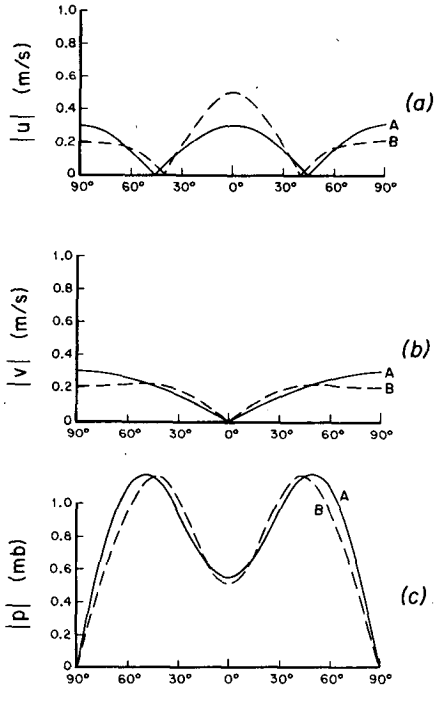

FIG. 4. Theoretical meridional structure of the $s = -1$, $n = 2$ planetary wave for $\epsilon \to 0$ (Example A) and $\epsilon = 10$ (Example B). Plots are magnitudes of (a) zonal velocity, (b) meridional velocity and (c) pressure.

3. Test for a static response to atmospheric pressure

a. Characteristics of the pressure field

The question of whether sea level at 4–6 days is responding statically to surface air pressure is nontrivial due to the existence of a narrow-band global atmospheric oscillation at the same periods. Madden and Julian (1972, 1973) firmly established the characteristics of an "equivalent-barotropic" oscillation of the atmosphere with a mean period of 5 days and zonal wavenumber $s = -1$ (westward propagating) cycles per circumference, extant at all longitudes and at latitudes from at least 60°N to 60°S. The observed mean wave characteristics (period, zonal wavenumber and meridional structure) were shown to be consistent with a solution to the Laplace tidal equations (LTE) found by Longuet-Higgins (1968). The solution is a wave of the second class (planetary or Rossby wave) with degree $n = 2$. When the period is 5 days, the Lamb parameter $\epsilon = (2\Omega a)^2/gh \approx 8.6$, so the equivalent depth $h \approx 10$ km, where g, a and Ω are defined as usual. Longuet-Higgins' (1968) numerical solution for the $s = -1$, $n = 2$ planetary wave with $\epsilon = 10$ is plotted in Fig. 4 (Example B). For comparison, the analytical solution for $\epsilon \to 0$ (Rossby-Haurwitz wave) is also shown (Example A). The frequency of the Rossby-Haurwitz wave is

$\omega \approx -2\Omega s(n^2 + n)^{-1}$, yielding a period of 3 days rather than the observed 5 days.

The power spectrum of sea level air pressure from Majuro Atoll (7°5'N, 171°23'E) is displayed in Fig. 5. The 5-day atmospheric wave produces a clear, although broad, peak in this spectrum. The peak is not always so obvious in surface pressure spectra because of frequently higher energy levels in the neighboring frequency bands. However, the oscillation is more narrow-band in wavenumber than the background and hence always produces high amplitude in air pressure coherence functions between stations separated by large distances (e.g., Fig. 6), except at high latitudes.

The high-resolution (maximum-likelihood) wavenumber spectrum of atmospheric pressure in the 4.6–6.0 day band, using two years of data from Canton, Johnston, Wake, Guam, Kwajalein and Eniwetok, is plotted in Fig. 7. The peak zonal wavenumber is $s \approx -1.6$, with 95% confidence interval of $-3.2 < s < 0$ and half-power bandwidth $\Delta s \approx 2.9$, which is consistent with previous estimates (Madden and Julian, 1972, 1973; Burpee, 1976). The peak meridional wavenumber is not significantly different from zero at even the 80% level (95% confidence interval is $-2.5 < m < 0.7$, where m is meridional wavenumber in cycles per circumference), as expected for an oscillation that is standing in latitude. The phases of the coherence functions for the station pairs separated by the largest distances uniformly imply (assuming no meridional propagation) that the zonal wavenumber is closer to -1 than -2 (e.g., Fig. 6).

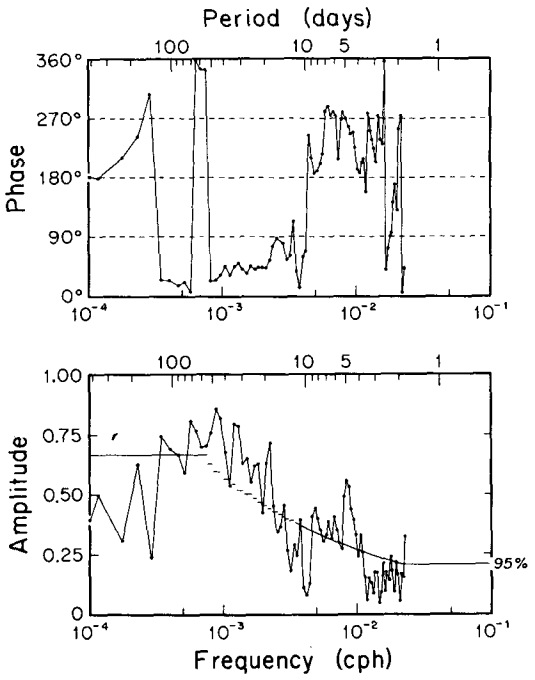

FIG. 6. Coherence amplitude and phase between seven years of surface air pressure from Canton Island (2°46'S, 171°43'W) and Balboa (8°57'N, 79°34'W), which are separated by more than 10 000 km. Note the large amplitude at 4–6 days due to the atmospheric wave; if $s = -1$ the phase should be 267°, and if $s = -2$ the phase should be 174°. Plotted as in Fig. 2.

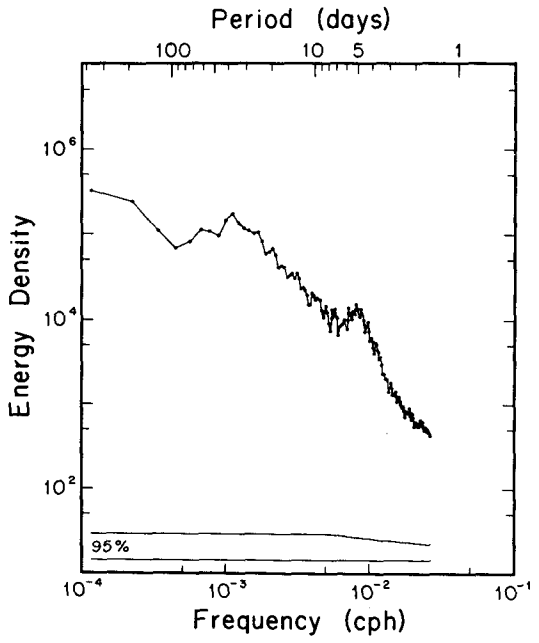

FIG. 5. Power spectrum of 18 years of surface air pressure from Majuro Atoll (7°5'N, 171°23'E). Note the broad peak at 5 days due to the "equivalent-barotropic" atmospheric wave. Note the broad peak at 5 days due to the "equivalent-barotropic" atmospheric wave. The ordinate is in units of (mb × 10)²/cph. Otherwise, plotted as in Fig. 1.

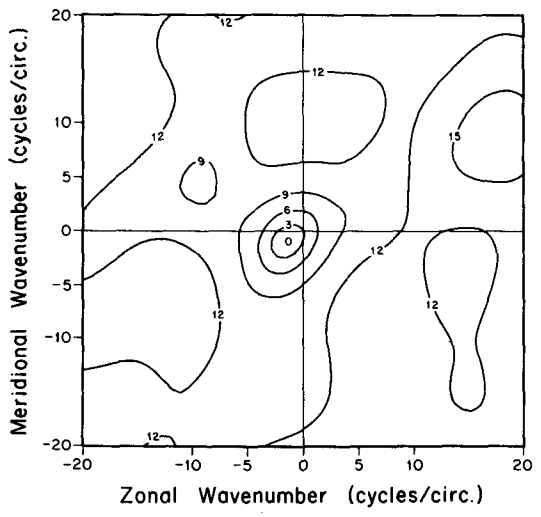

FIG. 7. Wavenumber spectrum of surface air pressure in the 4.6–6.0 day band using two years of data from Canton, Johnston, Wake, Gaum, Kwajalein and Eniwetok. The contours are power relative to the peak maximum, in negative decibels with the minus sign dropped. Peak is indicated by 0.

TABLE 2. Coherence and gain between sea level and surface air pressure in the 4–6 day band.

Station	Years of data	Coherence[a] Amplitude	Coherence[a] Phase[b]	Gain[a] (cm mb^{-1})
Balboa	6.5	$0.45^{+0.08}_{-0.11}$	−170 ± 11	1.31 ± 0.31
Galapagos	4.0	$0.46^{+0.08}_{-0.11}$	−150 ± 14	1.16 ± 0.34
Canton	16.5	$0.09^{+0.03}_{-0.05}$	137 ± 41	0.36 ± 0.17
Majuro	2.2	$0.23^{+0.09}_{-0.16}$	79 ± 44	0.57 ± 0.37
Kwajalein	4.0	$0.36^{+0.08}_{-0.11}$	117 ± 19	0.56 ± 0.19
Eniwetok	2.0	$0.34^{+0.10}_{-0.17}$	140 ± 29	0.51 ± 0.26
Truk	5.9	$0.39^{+0.07}_{-0.09}$	132 ± 14	0.63 ± 0.16
Yap	1.6	$0.50^{+0.12}_{-0.21}$	148 ± 23	0.83 ± 0.40
Guam	4.0	$0.48^{+0.08}_{-0.11}$	140 ± 14	0.63 ± 0.18
Wake	3.0	$0.39^{+0.10}_{-0.15}$	120 ± 22	0.43 ± 0.18
Johnston	5.6	$0.13^{+0.05}_{-0.12}$	41 ± 61	0.37 ± 0.36
Pago Pago	2.1	$0.36^{+0.11}_{-0.18}$	114 ± 28	0.79 ± 0.24
Hilo	3.8	$0.57^{+0.07}_{-0.10}$	162 ± 11	0.57 ± 0.13
Honolulu	11.3	$0.53^{+0.05}_{-0.07}$	159 ± 8	0.44 ± 0.09
Midway	4.0	$0.69^{+0.05}_{-0.07}$	161 ± 7	0.95 ± 0.15

[a] Error bars are the 95% confidence intervals (see Otnes and Enochson, 1972).

[b] Positive phase indicates sea-level leads. Phase is in degrees.

[For more convincing evidence of the mean wave characteristics (see Madden and Julian, 1972, 1973).]

The maximum amplitude of pressure occurs at midlatitudes (Fig. 4) where it probably averages 1 mb at the surface (Madden and Julian, 1973; Misra, 1975). The corresponding winds are too weak to be detected at sea level due to the existence of more energetic shorter scale (and widerband) processes, such as Rossby-gravity and easterly waves in the tropics (see Wallace, 1971; Shapiro, 1977; Luther, 1980) and storm systems at all latitudes. (N.b., the mean pressure fields associated with these processes are generally weaker than the barotropic oscillation at low latitudes but tend to obscure the barotropic oscillation at high latitudes.)

b. Sea level–air pressure relations

The coherences between sea level and air pressure in the 4–6 day band, for all the Pacific stations with co-temporal sea level and weather records, are given in Table 2. In addition, the complete coherence functions from Truk Atoll and the Galapagos Islands are plotted in Fig. 8. The coherence amplitude is high in the 4–6 day band (except at Canton, Majuro and Johnston), although the amplitude is typically not significantly different from the amplitudes at neigh-

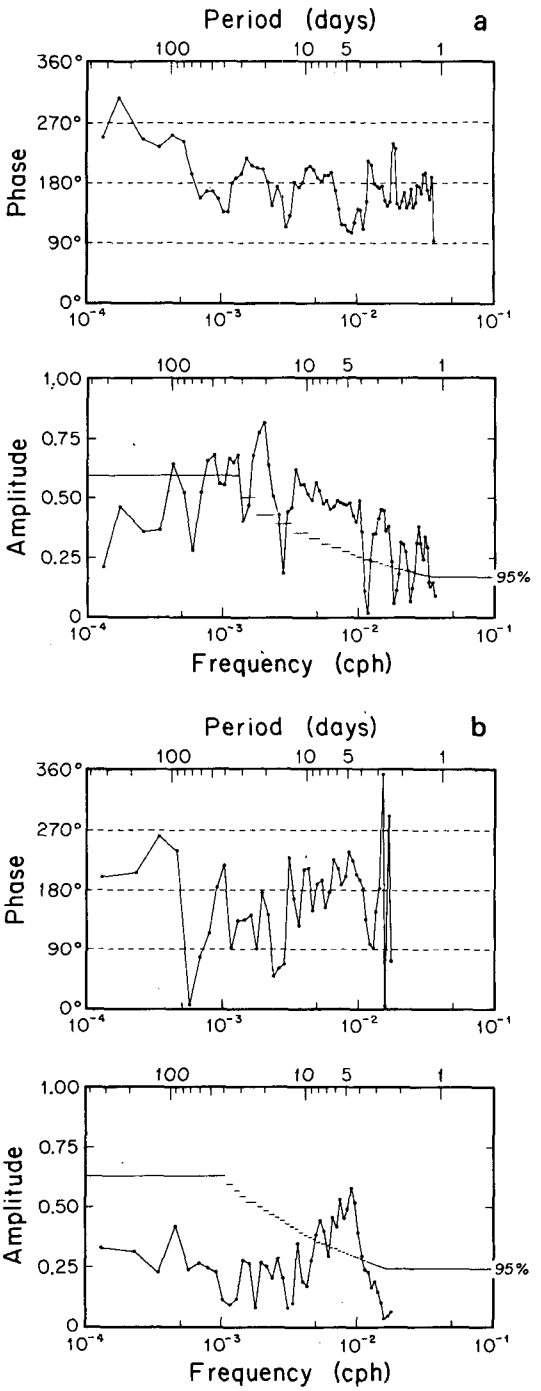

FIG. 8. Coherence amplitude and phase between sea level and atmospheric pressure for (a) 5.9 years of data from Truk Atoll (7°27′N, 151°52′E), and (b) 4 years of data from the Galapagos Islands (0°54′S, 89°34′W). The coherence amplitudes are strong in the 4–6 day band while the phase is not 180°, so sea level is not responding statically to air pressure. Positive phase indicates that sea level leads. Otherwise, plotted as in Fig. 2.

boring frequencies, as in Fig. 8a. What distinguishes the 4–6 day band is the coherence phase.

If the sea level response to air pressure is static, the phase should be 180° (i.e., the "inverted barometer" effect), but the phase is not 180° at 4–6 days (except perhaps at Balboa), while it almost always is at neighboring frequencies, as in Fig. 8a. Also, the gain is significantly different (at the 95% level) from the static 1.01 cm mb^{-1} at 10 of the 15 stations.

Of the three stations which show the lowest coherence between sea level and atmospheric pressure, two (Canton and Majuro) are within the equatorial waveguide, where sea level in the 4–6 day band is dominated by low-mode, equatorially-trapped, inertia-gravity waves and is coherent with surface winds (Wunsch and Gill, 1976; Luther, 1980). The fact that sea level, from the two remaining stations that are well within the equatorial waveguide (Truk and Galapagos), is coherent with air pressure (Fig. 8) and not the surface winds suggests that the low-mode, inertia-gravity waves decay from the central Pacific toward the meridional boundaries. Consistent with this interpretation, neither the Truk nor Galapagos sea level spectrum exhibits the narrow-band peaks associated with inertia-gravity waves, as at Christmas Island (Fig. 1). [For further details of the inertia-gravity wave field, see Luther (1980).]

The remaining station where sea level is only slightly coherent with air pressure (Johnston Island) has anomalously high sea level energy levels in the 1–30 day band compared with nearby Honolulu and Hilo and the more distant, but similar latitude, Wake Island. [This fact was first noted by Wunsch (1966).] The Johnston spectrum is quite similar to that from Midway Island, but Midway is much more coherent with air pressure. The origin of the "excess" energy at Johnston Island is unknown, but local island effects can be ruled out.

The coherences for Kwajalein, Eniwetok and Hilo in Table 2 are in excellent agreement with the sea-level–weather regressions computed by Groves and Hannan (1968) and Miyata and Groves (1971) using datasets that do not temporally overlap those used here. Both papers suggest the 4–6 day band is unusual in that sea level is coherent with atmospheric pressure yet does not respond statically.

Only sea level from Canton and Majuro is strongly coherent with surface winds in the 4–6 day band.

4. Possible barotropic, planetary basin mode(s)? A review

High coherence amplitudes between sea level records throughout the North Pacific in the 4–6 day band (e.g., Table 4, to be discussed later) negate the possibility that the oscillation is primarily baroclinic, since free baroclinic oscillations at those periods are necessarily confined to narrow equatorial or boundary waveguides (e.g., Philander, 1978). A plausible hypothesis at this point is that the oceanic oscillation is composed of one or more barotropic normal modes[1]

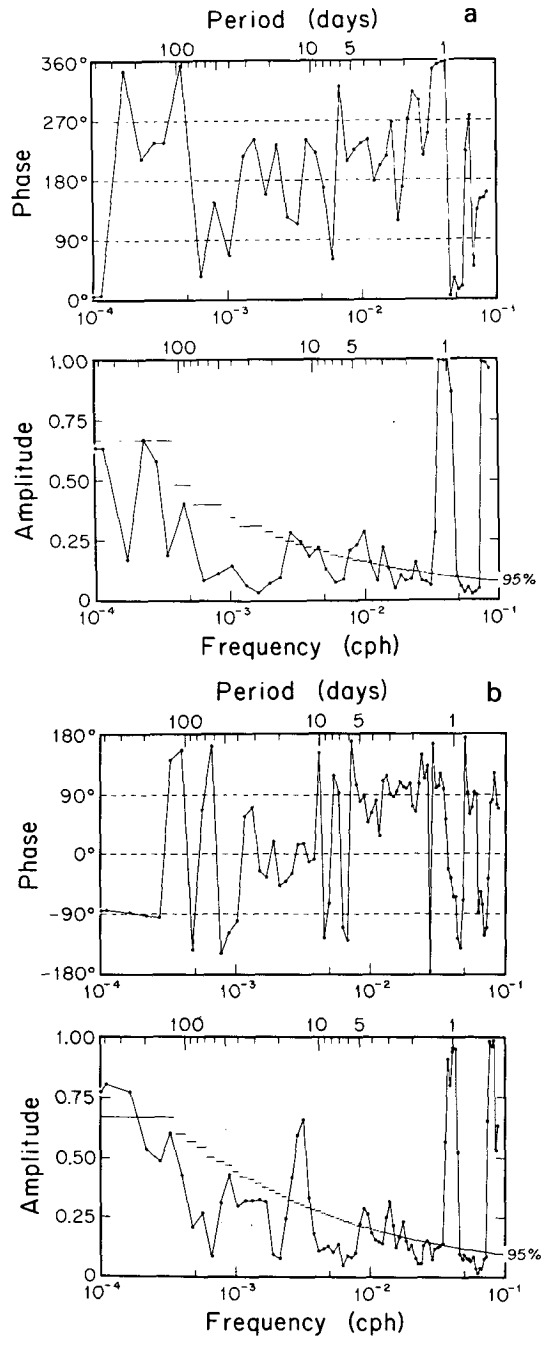

FIG. 9. Coherence amplitude between sea level records, showing significant (at the 95% level) amplitude in the 4–6 day band. The cause of the 3-day peak is unknown. Plotted as in Fig. 2. (a) Seven years from Honolulu (21°19'N, 157°52'W) and San Francisco (37°48'N, 122°28'W). The stations are separated by ~3900 km. (b) Seven years from Canton (2°49'S, 171°40'W) and Balboa (8°57'N, 79°34'W). The stations are separated by ~10 300 km.

[1] On the basis of a single sea level–air pressure coherence function, Wunsch and Gill (1976) postulated a "resonant barotropic response" at 5.4 days.

of the Pacific basin, probably planetary modes due to the long period. [The longest-period gravity mode computed by Platzman *et al.* (1981) for the Pacific has a period of 35.8 h.] Since sea level is coherent in the 4–6 day band over large distances (Fig. 9 and Table 4), the oceanic oscillation must be narrow-band in wavenumber, or, equivalently, the oscillation is composed of a small number of modes, probably only one.

The search for planetary waves in the Pacific began with Groves and Zetler's (1964) calculation of the coherence between sea level measured at Honolulu and San Francisco. Their results are in excellent agreement with Fig. 9a, but without further evidence they could not prove that the coherence in the 4–6 day band was due to "normal modes of long wavelength, or coherent weather." Groves and Hannan (1968) made a more determined attempt to find planetary waves in sea-level measurements from Kwajalein and Eniwetok. After removing the effects of local weather on sea level, they concluded that a small amount of planetary wave energy was present in the 5–10 day band. Longuet-Higgins (1966), in a classic numerical study of the planetary modes of a hemispherical basin centered at the equator, suggested that a small peak at two days period in the power spectrum of sea level at Honolulu (computed by Munk and Cartwright, 1966) was an indication of the gravest planetary mode of the Pacific Ocean. In a later note, referring to the sea-level coherence between Honolulu and Mokuoloe on the island of Oahu (computed by Miyata and Groves, 1968), Longuet-Higgins (1971) retracted this initial suggestion, but argued that peaks in the coherence at 2.9 and 4.3 days were possibly manifestations of the gravest planetary modes of the Pacific. The peaks could also be due to island-trapped waves, he noted. There is certainly no doubt that the peaks are not related to equatorially-trapped inertia-gravity waves which are miniscule at 10°N, let alone 21°N, the latitude of Honolulu, although this equatorial connection has been suggested (LeBlond and Mysak, 1978, p. 164).

The gravest planetary eigenmodes and eigenfrequencies for flat-bottom geometries which idealize the Pacific basin have been computed by several investigators. The eigenfrequencies for the lowest modes, from the most thorough analyses, are listed in Table 3. The gross differences in the model dynamics are indicated in the table. The spacing between modes is small, even for the gravest modes, and decreases for the higher modes.

Identification of the real ocean mode(s) responsible for the 4–6 day coherences in Figs. 2, 8 and 9, solely by matching the observed and theoretical frequencies, is impossible without a complete numerical solution with realistic geometry and topography, since the theoretical frequencies are sensitive functions of basin dimensions, depth and bottom slope. Longuet-Higgins (1965) found that for a midlatitude rectangular basin the frequency increased as any basin dimension increased. Therefore, in a later paper, Longuet-Higgins (1971) reduced the frequencies

TABLE 3. Eigenfrequencies of the gravest planetary modes in a homogeneous, flat-bottomed ocean with dimensions on the order of the Pacific.

	Longuet-Higgins (1966)		Longuet-Higgins & Pond (1970)	Rattray & Charnell (1966)	Mofjeld & Rattray (1971)
Basin geometry	Hemisphere	Circle[c]	Hemisphere	Rectangle[e]	Rectangle[f]
Rotational terms	$\Omega \times \hat{\mathbf{k}}$	β-plane	$\Omega \times \hat{\mathbf{k}}$	β-plane	β-plane
$\epsilon = (2\Omega a)^2/gD$	0	0	22[ad]	22	22
Periods (days) of gravest modes[b]					
Symmetrical					
1	3.3	2.4	4.5	4.1	4.2
2	4.1	3.3	5.0	4.9	5.0
3	5.0	4.5	5.6	6.0	6.1
Antisymmetrical					
1	1.6	1.5	2.0	2.7	2.6
2	2.6	2.4	2.9	3.8	3.8
3	3.6	3.5	3.8	5.1	5.2
4	4.6	4.5	4.7	5.3	5.6

[a] $\epsilon = 22$ corresponds to $h = 4$ km.

[b] Symmetry describes the structure of the surface displacement with respect to the equator. Ordering of the modes is on the basis of period.

[c] The basin is centered on the equator with radius = $\pi/2$ times the radius of the earth.

[d] Longuet-Higgins & Pond computed the frequencies for nearly all values of ϵ. We have chosen only the one value here for comparison with the other models.

[e] Zonal dimension is 1.3×10^4 km. Meridional extent is 6×10^3 km north of equator to 1.1×10^4 km south of equator.

[f] Basin is centered on the equator with zonal and meridional dimensions of 1.25×10^4 km.

of the gravest modes of a hemispherical basin [computed by Longuet-Higgins and Pond (1970)] by 30% to try to match the modes with the observation of sea level coherence between Honolulu and Mokuoloe. But Mofjeld and Rattray (1971) found that for a rectangular basin centered on the equator the frequency is also a strong function of the ratio of the two basin dimensions. The mode periods in Table 3 have not been adjusted for any differences between the model basin dimensions and the dimensions of the Pacific Ocean. Such an adjustment seems especially futile since topography (shelves, ridges, etc.) has been found to increase dramatically the frequencies of the planetary basin modes in numerical models (Christensen, 1973b; Platzman, 1975) and analytical studies (Ripa, 1978).

Indeed, topographic vortex stretching is usually so much stronger than planetary vortex stretching that it is hard to imagine that a basinwide planetary mode could exist in the real oceans. One expects the modes to be topographically controlled and so confined to regions much smaller than the basin dimensions. [This concept is clearly demonstrated in Willebrand *et al.*'s (1980) numerical studies, as mentioned in the Introduction.] However, the impressive computations by Platzman *et al.* (1981) of the normal modes of the world's oceans suggest that "hybrid" modes exist in the real rough-bottomed oceans. The "hybrid" modes have much of their energy trapped to a particular topographic feature yet have non-zero amplitude in the rest of the basin, where they generally have westward phase propagation. Unfortunately, Platzman *et al.* (1981) did not compute the modes for periods longer than 3⅓ days.

The models listed in Table 3 differ substantially in their choices of horizontal boundary conditions. Although the periods of the gravest modes are relatively insensitive to the boundary conditions (Buchwald, 1973; Flierl, 1977), the improper choice of boundary conditions may arbitrarily rule out possible solutions to the quasi-geostrophic equations, leading to misconceptions of the value of coastal observations. For instance, Longuet-Higgins (1971) dismisses the sea-level coherence (or lack thereof) between Honolulu and San Francisco [as computed by Groves and Zetler (1964), but see Fig. 9a] since "the vertical displacement is theoretically small" at San Francisco, but this theoretical result was due to the restrictive requirement that the streamfunction be zero on the horizontal boundaries (Longuet-Higgins, 1965). Larichev (1974) emphasized that since the theoretical planetary modes *can* have significant displacement at the boundaries, long records of sea level at coastal stations may be useful for studying the modes in the real oceans. Several coastal stations have been used in the present study.

5. Phase propagation of the oceanic wave

Table 4 lists the sea level coherence amplitudes and phases in the 3.5–6.0 day band for selected station pairs. This band was chosen so as to increase

TABLE 4. Coherence amplitude and phase between sea level records: (3.5–6.0 day band).

Station 1[a]	Station 2	Amplitude[b]	Phase[c] (deg)	Latitudinal separation (deg)	Longitudinal separation (deg)	Phase of[d] forced wave
Honolulu	Balboa	0.25	126 ± 33	12.4	78.3	−78 to −157
Canton	Balboa	0.24	73 ± 26	11.8	92.1	−92 to −184
Kwajalein	Canton	0.30	−13 ± 17	11.5	20.6	−21 to −41
Truk	Kwajalein	0.38	−8 ± 13	1.3	15.9	−16 to −32
Eniwetok	Canton	0.44	0 ± 27	14.2	26.0	−26 to −52
Yap	Truk	0.49	−11 ± 19	2.1	13.7	−14 to −27
Guam	Kwajalein	0.40	0 ± 15	4.7	23.1	−23 to −46
Guam	Eniwetok	0.50	−40 ± 26	2.1	17.7	−18 to −36
Guam	Wake	0.34	−26 ± 16	5.8	22.0	−22 to −44
Wake	Johnston	0.35	−31 ± 22	2.5	23.8	−24 to −48
Kwajalein	Honolulu	0.34	−98 ± 29	12.6	34.4	−34 to −69
Johnston	Hilo	0.26	−49 ± 24	3.0	14.5	−15 to −29
Canton	Honolulu	0.24	−52 ± 22	24.1	13.8	−14 to −28
Canton	Hilo	0.24	−62 ± 26	22.5	16.6	−17 to −33
Kwajalein	Pago Pago	0.35	−25 ± 33	23.0	21.6	−22 to −43
Pago Pago	Hilo	0.33	−27 ± 36	34.0	15.6	−16 to −31
Massacre Bay	Hilo	0.26	−50 ± 25	33.1	31.7	−32 to −63
Honolulu	San Francisco	0.26	−127 ± 20	16.5	35.4	−35 to −71
Hilo	San Francisco	0.27	−142 ± 18	18.1	32.6	−33 to −65
Massacre Bay	San Francisco	0.18	123 ± 28	15.0	64.3	−64 to −129

[a] Station 1 is always westward of station 2.

[b] Coherence amplitudes have not been corrected for bias, but all *are* significantly non-zero at the 95% level.

[c] Positive phase indicates first station leads second. Error bars are 95% confidence limits.

[d] This is the phase (in degrees) expected if the oceanic oscillations were solely the forced (i.e. static) response to the atmospheric forcing with zonal wavenumber $-2 < s < -1$.

the degrees of freedom in the coherence estimates after it was found that the phase changed only a small amount across this band. In general, the resolution of the original coherence computation was chosen to produce six independent estimates in the 3.5–6.0 day band. The estimates with significantly nonzero amplitudes (at the 90% level) were then vector-averaged to produce a final estimate, which appears in Table 4 if the amplitude is significantly nonzero at the 95% level. Coherences have not been computed for all combinations of station pairs, but only a representative sampling. In anticipation of the large zonal scale of the oscillation, only station pairs separated by more than 10° of longitude are included in Table 4. And finally, only station pairs with at least one station poleward of 8° from the equator are considered, in order to avoid "contamination" by equatorially-trapped inertia-gravity waves at 4–6 day periods. It should be mentioned that although the inertia-gravity waves dominate the sea-level spectra at 4–6 days in the central Pacific equatorial waveguide, they do so discontinuously (Fig. 1); in other words, the "background" between the inertia-gravity peaks is influenced by the barotropic mode. Hence cross-spectra between stations within the equatorial waveguide and those outside the waveguide can yield information on the barotropic mode (e.g., Fig. 9b). The most poleward stations in the dataset, Massacre Bay (~54°N) and Pago Pago (~14°S) are included in Table 4, supporting the idea that the oscillation is basin-wide.

To test again whether the oceanic oscillation is solely a forced response to the atmospheric forcing, the expected forced-wave phase differences between the stations, assuming that the forcing is westward-propagating with wavenumbers −1 to −2 (as discussed in Section 3a), are shown in Table 4. Ideally, we would like to have the actual phase differences of the forcing as computed from surface air pressure data, but we do not have enough data for this purpose; although, for example, the reader can compare the phase in Fig. 6 at 5 days with Table 4. The computed sea-level coherence phases are significantly different from the expected forced-wave phases for 45% of the station pairs shown. Although by itself not conclusive, this is another bit of evidence that the oceanic wave has free-wave components.

Planetary basin modes contain propagating as well as standing components. In β-plane models of planetary modes, the wavelength of the propagating component is always independent of latitude and mode, and the phase propagation direction is always westward. However, this is not the case for basins with non-constant β, in which higher modes have amphidromic points indicating eastward and meridional phase propagation in some regions. A consistent interpretation of the phases in Table 4 is that the oceanic wave has westward phase propagation with no nodes or amphidromes within the bounds of the dataset, analogous to the gravest symmetric mode of a hemispherical basin computed by Longuet-Higgins (1966; see Figure 7).[2] However, the coherences between Massacre Bay, Hawaii and San Francisco support equally well the possibility of an amphidrome to the north of Hawaii. Constructing phase diagrams at this time, therefore, seems premature.

6. Power spectra, amplitude and frequency-bandwidth estimates

The 4–6 day oceanic oscillation, which is clear in the coherences (Figs. 2, 8 and 9), is not a pronounced feature in the sea-level power spectra. This suggests that dissipation has smeared the frequency response into a broad frequency band, while the wavenumber bandwidth is narrow relative to the background noise, as for the 5-day atmospheric oscillation. Dissipation can be expected to skew the modal amplitude structure so that the strongest amplitudes are in the west, due to the different zonal scales of eastward and westward group velocity Rossby waves (Wunsch, 1967). In fact, some of the sea-level power spectra in the west Pacific do suggest a peak around 5 days; for instance, at Eniwetok Atoll in Fig. 10. [The 5.4 day peak at Eniwetok is definitely not due to equatorially-trapped inertia-gravity waves (Luther, 1980).] However, the sea-level spectrum at nearby Wake Island (also shown in Fig. 10) has only a slight "plateau" at 5.4 days, reflecting larger background energy levels at periods >5 days. Eniwetok and Wake are still strongly coherent at 4–6 days (Fig. 2).

Assuming the ocean is a linear system and that the frequency bandwidth of the power spectrum peak is the result of dissipation, the resonance quality, or Q (Munk and MacDonald, 1960), can be estimated. Using the spectra from Eniwetok Atoll (Fig. 10) and Guam (not shown), $Q \approx 4$. (Wunsch, 1972, estimated $Q \geq 3.3$ for a gravity mode of the North Atlantic.) The Q of the atmospheric forcing (Section 2) is also ~4 suggesting that this value should be considered an upper bound for the Q of the oceanic wave, since the bandwidth of the response is constrained to be less than or equal to the bandwidth of the forcing, if only a single oceanic mode is present. If more than one mode is present, the Q will have been underestimated, but the phases and significant amplitudes, at 4–6 days, of the coherence functions between sea-level records separated by large distances belie the presence of more than one mode.

The e-folding decay time of the energy in the 4–6 day ocean wave is $t_e \leqslant 3$ days, assuming $Q \leqslant 4$.

[2] Longuet-Higgins (1966) refers to the symmetry properties of the stream-function, whereas here we refer to the symmetry properties of sea-level displacement.

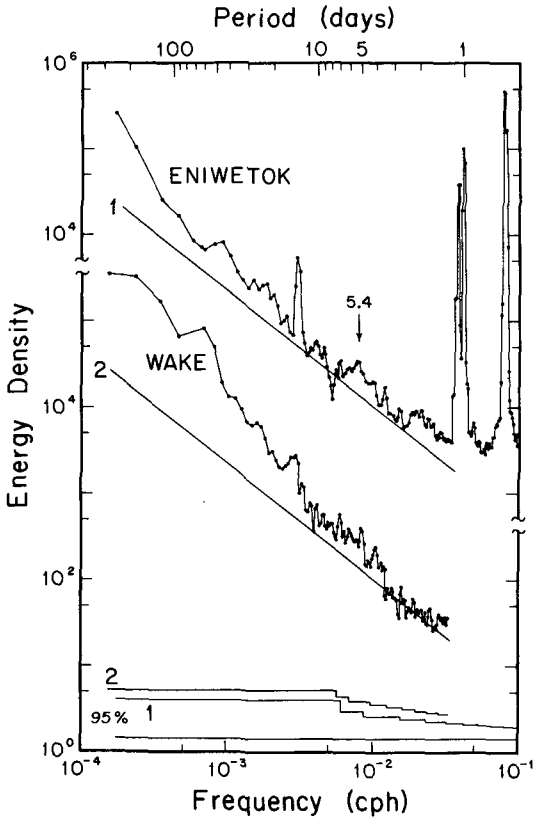

FIG. 10. Sea-level power spectra of 8.3 years of data from Eniwetok Atoll (11°21'N, 162°21'E) and 5.5 years of data from Wake Island (19°17'N, 166°39'E). Eniwetok, with a lower background level than Wake, has a peak, albeit broad, at ~5.4 days. This peak is not clearly present at Wake, although the energy level in the 4–6 day band is the same at both stations. The straight lines have −4/3 slopes, are separated by two orders of magnitude in their y intercepts and are intended solely for reference. Otherwise, plotted as in Fig. 1. See Fig. 2 for the coherence between these two stations.

Therefore, more than 80% of the wave's energy (55% of the amplitude) is lost per cycle. Although such large damping may seem to obviate the usefulness of describing the oceanic motion in terms of wave kinematics, in fact, oscillatory behavior is pronounced until the damping is closer to critical, which occurs when $Q = \frac{1}{2}$.

The root-mean-square amplitude of the 5.4-day "peak" at Eniwetok and Guam is ~0.4 cm, using a Q of 4. Groves and Hannan (1968) estimated that the planetary wave energy at ~5 days period at Kwajalein and Eniwetok corresponded to an rms sea-level amplitude of ~0.5 cm.

7. Summary of observations and deductions

Tropical sea-level fluctuations in the 4–6 day band are coherent with surface air pressure and incoherent with surface winds outside the central Pacific equatorial waveguide (~ ±8° and ~160°E to 100–130°W). Within the waveguide, sea level is coherent with surface winds and dominated by low-mode inertia-gravity waves.

The sea-level response to the atmospheric pressure forcing is non-static (i.e., not an "inverted barometer") as evidenced by sea level–air pressure coherence phases that are not 180°, sea level–air pressure gain amplitudes that are usually not 1.01 cm mb^{-1}, and inter-sea-level coherence phases that are frequently larger than expected for a purely forced wave.

The atmospheric forcing is in the form of a damped, "equivalent-barotropic", free planetary oscillation of the atmosphere with strong surface pressure field and weak surface wind fields. The wave structure is consistent with a global solution to the Laplace tidal equations that has a 5-day period, 10 km equivalent depth, zonal wavenumber $s = -1$ and degree $n = 2$ (Madden and Julian, 1972, 1973).

Significant coherence amplitudes in the 4–6 day band between sea-level records at all latitudes imply that the oceanic oscillation is barotropic. Significant coherence amplitudes over long distances imply that the oscillation is narrow band in wavenumber or, eqivalently, is composed of a small number of modes, probably only one.

The "free" wave component of the oscillation is probably a planetary wave, judging from the period and ubiquitous westward propagation. From the inter-sea-level coherence phases, the zonal wavelength of the propagating component varies between 7 000 and 30 000 km, if no meridional propagation is assumed.

The sea-level fluctuation in the west Pacific was found to have an rms amplitude of ~0.4 cm, with $Q \leqslant 4$ and, hence, an energy e-folding time $t_e \leqslant 3$ days.

8. Discussion, with caveats and plans

The actual horizontal structure of the 4–6 day oceanic oscillation is likely to be complex due to topography (see Platzman *et al.*, 1981). However, it is of some interest to note that the meridional amplitude structure of sea level for the gravest, symmetric mode of a flat-bottomed, hemispherical basin (Christensen, 1973a) is nearly identical to the forcing function pressure field described in Section 3 (Fig. 4).

As mentioned in Section 3, the surface air pressure fluctuations due to synoptic-scale weather systems obscure the "barotropic" atmospheric wave at mid-latitudes. Concomitantly, the sea-level response to the atmospheric wave tends to be obscured at high latitudes by the "static" sea-level response to the synoptic pressure fluctuations. It is possible that energy from the synoptic fluctuations ends up in the 4–6 day planetary oscillation of the Pacific, but this

is unlikely to be an important process because of the wide mismatch of horizontal scales and propagation directions at midlatitudes.

For the excitation of a normal mode of a linear system, the coherence phase between response and forcing is expected to pass through 180° as the frequency of the forcing crosses the resonance frequency. That this does not occur in the sea level–air pressure coherences at 4–6 days (e.g., Fig. 8) could be due to the fact that the background sea level energy is coherent with air pressure and has a uniform phase of 180° (Fig. 8a). Similarly, the oceanic response itself can have an important "forced" component which contributes a uniform phase (in this case, 180°) to the sea level-air pressure coherences. The relative energies in the "forced" and "free" components of the 4–6 day oceanic oscillation have not been determined.

The energy decay time, $t_e \leqslant 3$ days, found for the oceanic oscillation is much shorter than values typically found in analytical and numerical studies of the strength of atmospherically forced planetary oscillations. For instance, Müller and Frankignoul (1981) employ a scale-independent damping that corresponds to an energy decay time of $t_e = 100$ days. With stronger damping, corresponding to $t_e = 3$ days, the atmospherically forced oscillations computed by Müller and Frankignoul (1981) would be insignificant compared with observed energy levels in the ocean. It is, of course, unlikely that the damping is scale-independent or that baroclinic oscillations will be heavily damped. The curiosity is why the 4–6 day oceanic oscillation, with such a large horizontal scale, is so strongly attenuated. Bottom drag and lateral diffusion (using typical values for the friction coefficients) cannot produce such a short decay time. Perhaps topographic wave drag is an important process.

In retrospect, the dataset used here is quite inadequate for studying a basin-wide oscillation, not just because of the non-uniform distribution of island platforms, but also because of the lack of coastal data. Some of the observations, such as the lack of nodes and amphidromes, are suspect due to the paucity of data. To remedy this situation, more coastal (and island) tide-gage and weather records are being assembled. It should be possible to produce co-phase maps of the 4–6 day oceanic oscillation. Application of the seismological "stacking" techniques (Buland *et al.*, 1979) should improve estimates of amplitude and Q.

Acknowledgments. It is a pleasure to acknowledge many beneficial discussions with Professor Carl Wunsch. I would also like to thank K. O'Neill for critically reviewing the manuscript and D. Betts for assistance on the graphics. This work began as part of the author's Ph.D. dissertation in the Joint Program in Oceanography of the Massachusetts Institute of Technology and the Woods Hole Oceanographic Institution. Support was provided by NSF Grant OCE 73-01384 and ONR Contract N00014-C-75-0291 at M.I.T., and NSF Grant OCE 78-23134 at Scripps Institution of Oceanography.

REFERENCES

Bingham, C., M. D. Godfrey and J. W. Tukey, 1967: Modern techniques of power spectrum estimation. *IEEE Trans. Audio Electroacoust.*, **AU-15,** 56–66.

Buchwald, V. T., 1973: Long-period divergent planetary waves. *Geophys. Fluid. Dyn.*, **5,** 359–367.

Buland, R., J. Berger and F. Gilbert, 1979: Observations from the IDA network of attenuation and splitting during a recent earthquake. *Nature,* **277,** 358–362.

Burpee, R. W., 1976: Some features of global scale 4–5 day waves. *J. Atmos. Sci.*, **33,** 2292–2299.

Capon, J., 1969: High-resolution frequency-wavenumber spectrum analysis. *Proc. IEEE,* **57,** 1408–1418.

——, and N. R. Goodman, 1970: Probability distributions for estimators of the frequency-wavenumber spectrum. *Proc. IEEE,* **58,** 1785–1786.

Christensen, N. Jr., 1973a: On free modes of oscillation of a hemispherical basin centered on the equator. *J. Mar. Res.*, **31,** 168–174.

——, 1973b: The effect of a coastal shelf on long waves in a rotating hemispherical basin. *J. Mar. Res.* **31,** 175–187.

Flierl, G. R., 1977: Simple applications of McWilliams' "A note on a consistent quasigeostrophic model in a multiply connected domain." *Dyn. Atmos. Oceans,* **1,** 443–453.

Frankignoul, C., and P. Müller, 1979: Quasi-geostrophic response of an infinite β-plane ocean to stochastic forcing by the atmosphere. *J. Phys. Oceanogr.*, **9,** 104–127.

Groves, G. W., and E. J. Hannan, 1968: Time series regression of sea level on weather. *Rev. Geophys.*, **6,** 129–174.

——, and B. D. Zetler, 1964: The cross spectrum of sea level at San Francisco and Honolulu. *J. Mar. Res.*, **22,** 269–275.

Harrison, D. E., 1979: On the equilibrium linear basin response to fluctuating winds and mesoscale motions in the ocean. *J. Geophys. Res.*, **84,** 1221–1224.

Hendry, R., and C. Wunsch, 1973: High Reynolds number flow past an equatorial island. *J. Fluid Mech.* **58,** 97–114.

Hogg, N., 1972: Steady flow past an island with application to Bermuda. *Geophys. Fluid Dyn.*, **4,** 55–81.

Hwang, H. J., 1970: Power density spectrum of surface wind speed on Palmyra Is. *Mon. Wea. Rev.*, **98,** 70–74.

Larichev, V., 1974: Statement of an internal boundary problem for the Rossby wave equation. *Izv. Atmos. Ocean. Phys.*, **10,** 470–473.

Larsen, J. C., 1977: Cotidal charts for the Pacific Ocean near Hawaii using f-plane solutions. *J. Phys. Oceanogr.*, **7,** 100–109.

LeBlond, P. H., and L. A. Mysak, 1978: *Waves in the Ocean.* Elsevier Scientific, 602 pp.

Leetmaa, A., 1978: Fluctuating winds, an energy source for mesoscale motions. *J. Geophys. Res.*, **83,** 427–430.

Longuet-Higgins, M. S., 1965: Planetary waves on a rotating sphere II. *Proc. Roy. Soc. London,* **A284,** 40–54.

——, 1966: Planetary waves on a hemisphere bounded by meridians of longitude. *Phil. Trans. Roy. Soc. London,* **A260,** 317–350.

——, 1968: The eigenfunctions of Laplace's tidal equations over a sphere. *Phil. Trans. Roy. Soc. London,* **A262,** 511–607.

——, 1971: On the spectrum of sea level at Oahu. *J. Geophys. Res.*, **76,** 3517–3522.

——, and G. S. Pond, 1970: The free oscillations of fluid on a

hemisphere bounded by meridians of longitude. *Phil. Trans. Roy. Soc. London,* **A266,** 193–223.

Luther, D. S., 1980: Observations of long period waves in the tropical oceans and atmosphere. Ph.D. dissertation, Joint Program in Oceanography, Massachusetts Institute of Technology and the Woods Hole Oceanographic Institution, 210 pp.

——, and C. Wunsch, 1975: Tidal charts of the central Pacific Ocean. *J. Phys. Oceanogr.,* **5,** 222–230.

Madden, R. A., and P. R. Julian, 1971: Detection of a 40–50 day oscillation in the zonal wind in the tropical Pacific. *J. Atmos. Sci.,* **28,** 702–708.

——, and ——, 1972: Further evidence of global scale, 5-day pressure waves. *J. Atmos. Sci.,* **29,** 1464–1469.

——, and ——, 1973: Reply. *J. Atmos. Sci.,* **30,** 935–940.

Matsuno, T., 1966: Quasi-geostrophic motions in the equatorial area. *J. Meteor. Soc. Japan,* **44,** 25–42.

Misra, B. M., 1975: Evidence of the 5-day period oscillations in the geopotential field. *Tellus,* **27,** 469–483.

Miyata, M., and G. W. Groves, 1968: Note on sea level observations at two nearby stations. *J. Geophys. Res.,* **73,** 3965–3967.

——, and ——, 1971: A study of the effects of local and distant weather on sea level in Hawaii. *J. Phys. Oceanogr.,* **1,** 203–213.

Mofjeld, H. O., and M. Rattray, Jr., 1971: Free oscillations in a beta-plane ocean. *J. Mar. Res.,* **29,** 281–305.

Moore, D. W., and S. G. H. Philander, 1977: Modelling of the tropical oceanic circulation. *The Sea,* Vol. 6, Wiley, 319–361.

Müller, P., and C. Frankignoul, 1981: Direct atmospheric forcing of geostrophic eddies. *J. Phys. Oceanogr.,* **11,** 287–308.

Munk, W. H., and D. E. Cartwright, 1966: Tidal spectroscopy and prediction. *Phil. Trans. Roy. Soc. London,* **A259,** 533–581.

——, and G. J. F. MacDonald, 1960: *The Rotation of the Earth.* Cambridge University Press, 323 pp.

Otnes, R. K., and L. Enochson, 1972: *Digital Time Series Analysis.* Wiley, 467 pp.

Philander, S. G. H., 1978: Forced oceanic waves. *Rev. Geophys. Space Phys.,* **16,** 15–46.

Phillips, N., 1966: Large-scale eddy motion in the western Atlantic. *J. Geophys. Res.,* **71,** 3883–3891.

Platzman, G. W., 1975: Normal modes of the Atlantic and Indian Oceans. *J. Phys. Oceanogr.,* **5,** 201–221.

Platzman, G. W., G. A. Curtis, K. S. Hansen and R. D. Slater, 1981: Normal modes of the world ocean. Part II. Description of modes in the period range 8 to 80 hours. *J. Phys. Oceanogr.,* **11,** 579–603.

Ramage, C. S., C. W. Adams, A. M. Hori, B. J. Kilonsky and J. C. Sadler, 1980: *Meteorological Atlas of the 1972–73 El Niño.* University of Hawaii, Department of Meteorology Publ. UHMET 80-03.

Rattray, M. Jr., and R. L. Charnell, 1966: Quasi-geostrophic free oscillations in enclosed basins. *J. Mar. Res.,* **24,** 82–102.

Rhines, P., and F. Bretherton, 1973: Topographic Rossby waves in a rough-bottomed ocean. *J. Fluid Mech.,* **61,** 583–607.

Ripa, P., 1978: Normal Rossby modes of a closed basin with topography. *J. Geophys. Res.,* **83,** 1947–1957.

Shapiro, L. J., 1977: Tropical storm formation from easterly waves: A criterion for development. *J. Atmos. Sci.,* **34,** 1007–1021.

Wallace, J. M., 1971: Spectral studies of tropospheric wave disturbances in the tropical western Pacific. *Rev. Geophys. Space Phys.,* **9,** 557–612.

Willebrand, J., S. G. H. Philander and R. C. Pacanowski, 1980: The oceanic response to large-scale atmospheric disturbances. *J. Phys. Oceanogr.,* **10,** 411–429.

Wunsch, C., 1966: On the scale of the long period tides. Ph.D. dissertation, Massachusetts Institute of Technology, 147 pp.

——, 1967: The long-period tides. *Rev. Geophys.,* **5,** 447–475.

——, 1972: Bermuda sea level in relation to tides, weather and baroclinic fluctuations. *Rev. Geophys. Space Phys.,* **10,** 1–49.

——, and A. E. Gill, 1976: Observations of equatorially trapped waves in Pacific sea level variations. *Deep-Sea Res.,* **23,** 371–390.

——, and R. Hendry, 1972: Array measurements of the bottom boundary layer and the internal wave field on the continental slope. *Geophys. Fluid Dyn.,* **4,** 101–145.

Wyrtki, K., and G. Meyers, 1975: The trade wind field over the Pacific Ocean. Part I: The mean field and the mean annual variation. Hawaii Institute of Geophysics, University of Hawaii, Rep. HIG-75-1, 55 pp.